ELSEVIER

Ceramics International 25 (1999) 383–387

CERAMICS INTERNATIONAL

The influence of B_2O_3 on the sintering of MgO–CaO–Al_2O_3–SiO_2 composite glass powder

Cheng-Fu Yang [a,*], Chien-Min Cheng [b]

[a] *Department of Electronic Engineering, Chinese Air Force Academy, PO Box 90277-4, Kangshan, Kaohsiung, Taiwan 82012*
[b] *Department of Electronic Engineering, Nan-Tai Institute of Technology, 1, Nan-Tai St, Yung Kang, Tainai, Taiwan*

Received 12 January 1998; accepted 12 May 1998

Abstract

B_2O_3 has been found to be a useful flux to densify the MgO–CaO–SiO_2–Al_2O_3 (MCAS) composite glass powders, which are obtained by the sol–gel method. The temperatures needed to fully densify MCAS decrease with increase of B_2O_3 addition. For MCAS with different amounts of B_2O_3 addition, no apparently exothermic peaks are associated to the glass crystallization and the polymorphic transformation of μ-cordierite to the α-form. The softening temperature (T_s) of MCAS glass decreases with the increase of B_2O_3 additive. For MCAS with 6 wt% B_2O_3 added, only one broad endothermic peak associated T_s is observed in the differential thermal analysis curve. For the same sintering temperature, as the amount of B_2O_3 addition increases, the crystallization rates of anorthite and cordierite firstly increase, after reaching a maximum (900°C for 3 wt%, 930°C for 1 wt%), and then decrease. Too much B_2O_3 is not necessary because it inhibits the cordierite and anorthite crystallization.

Keywords: D. Glass; D. Cordierite; Sol–gel; Endothermic peak; Crystallization; Anorthite

1. Introduction

Cordierite ($2MgO–2Al_2O_3–5SiO_2$) and cordierite-based glass ceramics are promising materials for electronic packaging because they have a low dielectric constant (5.0 at 1 MHz), a low thermal expansion coefficient (about $30\times10^{-7}/°C$), and good electrical insulation [1,2]. There were two common routes to form glass articles, one was the glass-ceramics process [3,4] and the other the reactive 'sol–gel' process [5,6]. Recently, pure and crystalline cordierite powders and cordierite-based glass were prepared by the sol–gel method [5–8]. The sol–gel process attempted to duplicate the mixing levels of the melt process by simultaneous precipitation of the appropriate metal species as hydroxides and then dehydrating them to yield intimately mixed oxides [7]. Using sol–gel techniques, chemical homogenization glasses and glass composite formation can be achieved in solution near room temperature.

On sintering cordierite-glass powders, a stoichiometric cordierite glass composition is difficult to sinter unless it is in the composition range that contains more MgO and less Al_2O_3 than stoichiometric cordierite. Another method of improving the sinterability of stoichiometric cordierite glass powders is the addition of sintering aids. In the past, Cr_2O_3, CeO_2, ZrO_2, and K_2O have been used [9–11]. Kumar et al. [12] and Kondo et al. [9] applied B_2O_3-added cordierite glass ceramics to fabricate multilayer substrate [9]. In this study, glass with composition in the quaternary primary phase field of the MgO–CaO–Al_2O_3–SiO_2 (abbreviated as MCAS) system was prepared by a sol–gel method [2,7]. Doping B_2O_3 was chosen for its low melting point and less harmful effect on the insulating characteristics than the other sintering aids [9,12]. We used the MCAS glass powder as the precursor to prepare dense cordierite-based ceramics and develop its sintering characteristics at less than 1000°C. The influence of B_2O_3 on the sintering characteristics of MCAS glass ceramics is developed in this paper.

2. Experimental procedures

In the work reported here, a homogeneous glass of the basic composition (in wt%): MgO5%, CaO19%,

* Corresponding author. Fax: +886-7-395-0045; e-mail: grouse@cc.cafa.edu.tw

0272-8842/99/$20.00
PII: S0272-8842(98)00049-2

$Al_2O_3$26%, and $SiO_2$50% (with an approximate stoichiometry of MgO:CaO:Al_2O_3:SiO2 = 6.5:14.5:27.5:51.5) were prepared by the sol–gel method. In a typical laboratory scale synthesis using the nitrates, colloidal silica was dispersed in 600 ml of a solution of deionized water, and concentrated nitric acid was also added to the solution. To this acidic suspension we added magnesium nitrate hexahydrate, aluminum nitrate hexahydrate, and calcium nitrate hexahydrate. The subsequent addition of ammonium hydroxide resulted in the quantitative precipitation of magnesium, calcium, and aluminum hydroxides. The solids were collected by filtration and calcined at 300°C for 1 h. The calcination step was desirable to convert any ammonium nitrate present to oxides of nitrogen and water. The resulting material was the MCAS glass precursor. MCAS composite powders containing 0, 1, 3, and 6% by weight of B_2O_3 were prepared by a slurry method; these powders will hereafter be referred to as MCASB0, MCASB1, MCASB3, and MCASB6, respectively. The powder was dried, ground, and pressed to pellets uniaxially in a steel die. Typical dimensions of the pellets were 15 mm in diameter and 1.5 mm in thickness. Pellets were fired in air from room temperature at a rate of 5°C/min to a sintering temperature (from 800 to 1000°C), followed by a 40 min hold.

The microstructure observations of the surfaces of sintered specimens were done on a scanning electron microscope (SEM). The crystalline structures of sintered MCAS glass ceramics were investigated using X-ray diffraction (XRD) patterns. The densities of sintered specimens as a function of sintering temperature were measured by the liquid displacement method (Archimedes method). The shrinkage of sintered specimens was measured by a digital meter. Glass powders with different amounts of B_2O_3 additive were analyzed by differential thermal analysis (DTA) to find the ranges of softening and crystallization temperatures. The range of testing temperature was from 300 to 1200°C with a heating rate 10°C/min.

3. Results and discussion

SEM observations on B_2O_3 added specimens sintered at 930°C are shown in Fig. 1(a)–(c), with the addition of 0, 3, and 6 wt% B_2O_3, respectively. The coalescence of glass particles was easily seen in Fig. 1(a) for MCASB0. For MCASB3, pore elimination and the enhancement of densification were promoted by the viscous flow of B_2O_3 as shown in Fig. 1(b). Viscous flow of the flux coalesced the glass particles and densification becomes more complete as the amount of B_2O_3 rises. As Fig. 1(c) shows that for MCASB6 densification is more apparent and fewer pores are recognized.

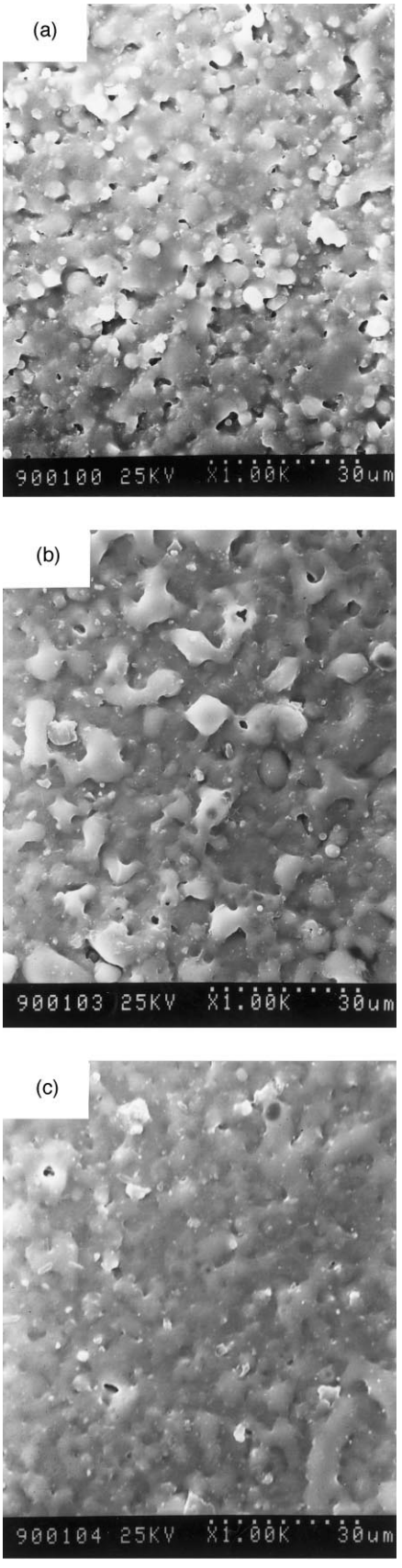

Fig. 1. The SEM micrograph of sintered B_2O_3–MCAS glass ceramics: (a) 0 wt%, (b) 3 wt%, and (c) 6 wt%. Sintering temperatures = 930°C.

The densification of MCAS glass ceramics, added with different amounts of B_2O_3 and sintered at different temperatures, is shown in Fig. 2. The sinterability of MCAS composite glass was poorer than those of B_2O_3-added MCAS glass. During the initial sintering of MCASB0 compacts, densification started at about 840°C. The density increased with temperature and went to saturation at about 930°C. As the content of B_2O_3 increased, a much easier densification of the glass compacts was evidenced in Fig. 2, and rapid densification occurred at the lower temperature. Easier densification of MCAS specimens added with more B_2O_3 may be due to the flux effect of B_2O_3 which enhances the densification during sintering. With liquid formation, there was a rapid densification due to capillary force exerted by the liquid on the particles.

Because of the low melting point of B_2O_3, the procedure of sintering MCAS glass would be a reactive liquid-phase sintering process. The viscosity of MCAS glass was determined by the amounts of added B_2O_3 and heat treatment temperature. Since the viscosity was inversely proportional to the sintering temperature, higher sintering temperature resulted in easier densification. In sintering B_2O_3-added MCAS glass ceramics, Newtonian viscosity flow was found to be the predominant mechanism [13]. The kinetics for the initial stages of sintering are described as follows:

$$\Delta L/L = (3\gamma/4r\eta)^{*}t, \tag{1}$$

where $\Delta L/L$ is the shrinkage ratio of the sintered MCAS composites, γ is the surface tension, η is the viscosity. Value of surface tension is about 0.3 to 0.35 for silicate glass, and about 0.3 for cordierite glass [14]. Although surface tension is a function of temperature, the change of surface tension is small and can essentially be considered as a constant. The relationships between viscosity and temperature can be well described by the Fulcher equation [15], whereas, over short temperature ranges, an Arrhenius equation is adequate and can be expressed as follows [16]:

$$\ln\eta = \ln\eta_o + C_1/T = C_2 + C_1/T, \tag{2}$$

where C_1 is a constant and T is the temperature in Kelvin. After substituting Eq. (2) into Eq. (1), the following equation is obtained:

$$\ln(\Delta L/L) = \ln(3\gamma t/4r) - \ln\eta_o - C_1/T = C_3 - C_1/T \tag{3}$$

For the case where the sintering time and the radius of particle are essentially the same, C_3 can be considered as a constant. Plots of ln $(\Delta L/L)$ versus $1000/T$ for MCAS glass with different amounts of B_2O_3 added are shown in Fig. 3. For MCASB0, Eq. (3) is applied well to a wider range of temperatures; for MCASB3 and MCASB6, it is applied only to a narrower range. The departure from Eq. (3) means that the Newtonian viscous flow is no longer a predominant mechanism for sintering B_2O_3-added MCAS under the temperatures in consideration in Fig. 3. However, the Frankel viscous flow sintering model [14] alone is not enough to explain the sintering kinetics of B_2O_3-added MCAS glass compacts in this work. One possible reason is the earlier completion of densification resulting from the addition of B_2O_3, which accelerates the densification of MCAS glass. Another reason might be the crystallization of cordierite and anorthite (for that will be demonstrated in Fig. 4), because the onset of crystallization results in an abrupt increase in the viscosity [17].

The X-ray diffraction patterns of MCAS glass powder with different amounts of B_2O_3 addition

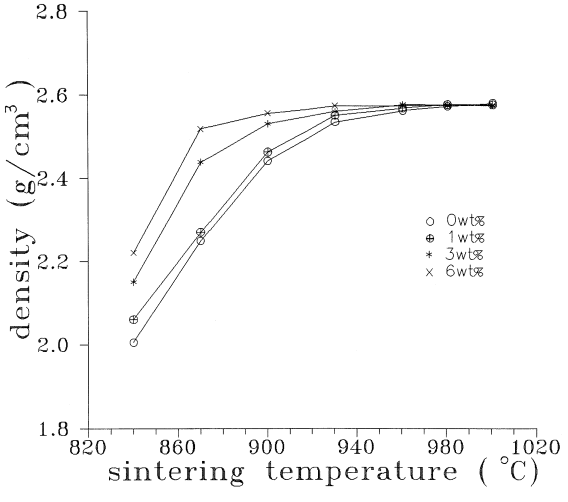

Fig. 2. The densities of MCAS glass ceramics as a function of sintering temperature and B_2O_3 amount.

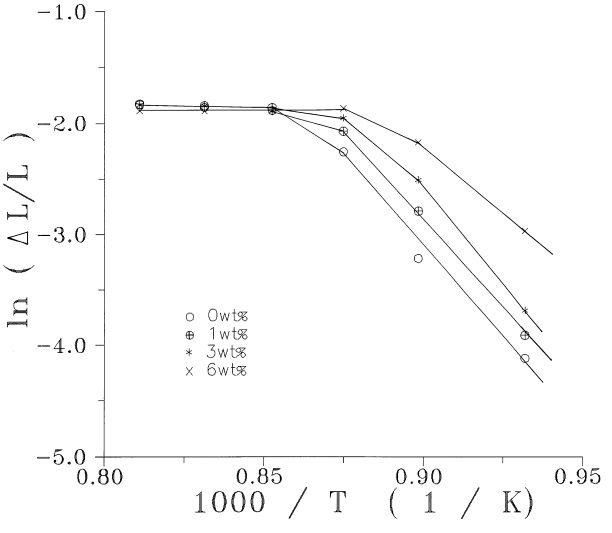

Fig. 3. Plot of $\ln(\Delta L/L)$ versus $1000/T$ for sintered B_2O_3-added MCAS.

isothermally treated at various temperatures are shown in Fig. 4. At 870°C sintering temperature, all the fired samples showed neither cordierite nor anorthite, although the sample had partially densified. The MCAS glass with different amounts of B_2O_3-added and sintered at 900 and 930°C are shown in Fig. 4(a) and (b). The crystallization rates of cordierite and anorthite were both of sintering temperature and B_2O_3 concentration dependent. The crystallization rates of cordierite and anorthite increased (0∼3 wt% for 900°C, 0∼1 wt% for 930°C), reached a maximum value, and then decreased (3∼6 wt% for 900°C, 1∼6 wt% for 930°C) with B_2O_3 concentration. At 900°C, the liquid-phase sintering process effect of B_2O_3 was more pronounced; because the crystallization rates of cordierite and anorthite increased with the amount of B_2O_3 addition up to 3 wt%. For 930°C, because of the increased flux of MCAS glass, the highest crystallization rates of cordierite and anorthite were shifted to MCAS1. As Fig. 4 shows, too much B_2O_3 (6 wt%) is not necessary, because too much inhibits the crystallization of cordierite and anorthite. To inspect the existing crystalline structure under each sintering temperature, the metastable μ-cordierite and β-quartz did not appear in the sintered MCAS glass ceramics. The high temperature stable α-cordierite was the main crystalline structure.

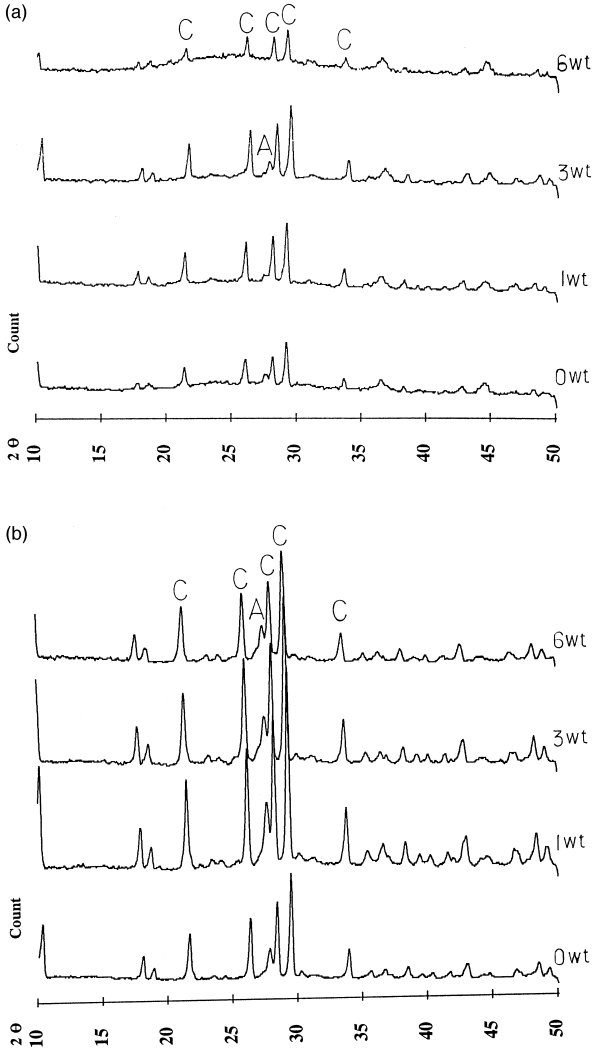

Fig. 4. X-ray diffraction patterns of MCAS composites glass sintered at (a) 900°C and (b) at 930°C (A, anorthite; C, cordierite).

The differential thermal analysis (DTA) records of MCAS glass powders with different amounts of B_2O_3 addition are shown in Fig. 5. For MCASB0, two apparently endothermic peaks centered at 930 and 1020.5°C and one small endothermic peak centered at 981.5°C are observed. The endothermic peak at about 930°C in MCASB0 is sharp and distinct, while it was shifted to the lower temperature as the amount of B_2O_3 increased. For MCASB3, the two apparent endothermic peaks are shifted to 926.5 and 1013.5°C and the one small endothermic peak was shifted to 979.5°C. For MCAS6, only one broad endothermic peak was observed. For MCAS with different amounts of B_2O_3 added, no apparent exothermic peaks associated to cordierite and anorthite crystallization were observed in the DTA curves. Apparently the broad endothermic peaks in Fig. 5 were associated with the softening point of the MCAS–B_2O_3 system. The endothermic peaks in MCASB0 were sharp and distinct, while it was shifted to lower temperature, diffused, and broad for MCASB6.

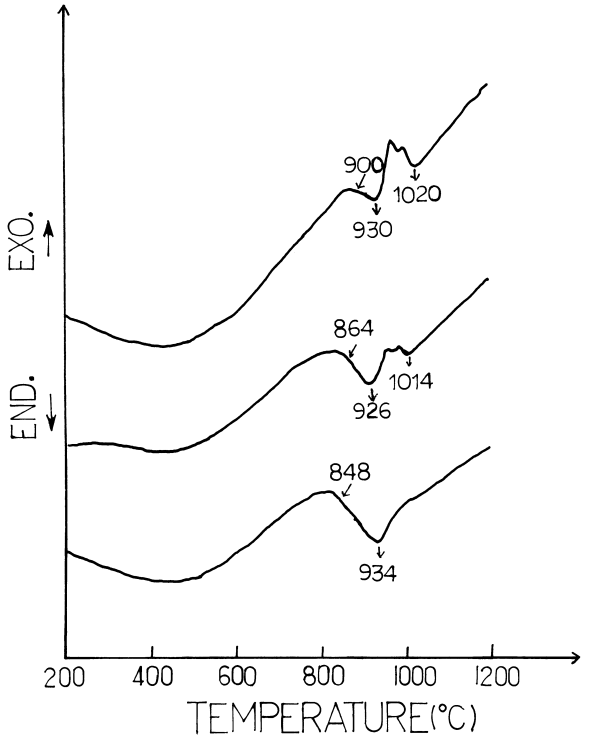

Fig. 5. DTA records of MCAS glass with different amounts of B_2O_3 addition. Upper line for MCASB0, middle line for MCASB3, and lower line for MCASB6.

Table 1
The softening temperature of B_2O_3-added MCAS glass

Composition	Estimated value (°C) [from Eq. (4)]	Tested value (°C) (from DTA)
MCAS + 0 wt% B_2O_3	846.1	900
MCAS + 3 wt% B_2O_3	842.4	880
MCAS + 6 wt% B_2O_3	838.9	848

These results suggest again that the procedure of sintering B_2O_3-added MCAS glass would be a reactive liquid-phase sintering process involving the dissolution of all the oxides starting materials in the flux, where reaction would occur followed by precipitation of a crystalline product from the flux.

The choice of B_2O_3 is not only for its low softening point but also its properties have been well studied [18]. Glass softening temperature (T_s), dielectric constant, and thermal expansion coefficient can be accommodated within the glass composition ranges. Properties of B_2O_3 added MgO–CaO–Al_2O_3–SiO_2 can be predicted by a linear equation form as follows [18]:

$$P_i = Zr_i w_i + I_p, \tag{4}$$

where P_i is the property in equation (T_s), r_i is the unstandardized regression coefficient for each component i, w_i is the weight per cent associated with that component, and I_p is an intercept value. More actual value of softening temperature T_s in the B_2O_3–MgO–CaO–Al_2O_3–SiO_2 system is [18]:

$$T_s(^\circ\mathrm{C}) = -1.14B_2O_3 + 0SiO_2 - 1.32Al_2O_3 + 1.08CaO + 5.5MgO + 832.4, \tag{5}$$

where the component concentrations are in weight per cent. By changing the component concentration of each oxide, the expected value of T_s can be obtained. Table 1 compares the estimated softening temperature [from Eq. (4)] and the tested softening temperature (from Fig. 5). It was found that the tested values were lower than estimated values. The tested values also shifted to lower temperature as the amount of B_2O_3 addition increased. The causes of the large temperature difference between the tested values and the estimated values could not be identified.

4. Conclusions

1. The sintering density increases with the sintering temperature, but the addition of B_2O_3 has no apparent influence on saturated density of MCAS ceramics. The density of sintered nonporous MCAS specimens is about 2.580 g/cm^3.
2. The temperatures needed to densify MCAS glass ceramics decrease with increase in the amounts of B_2O_3 additive, but too much B_2O_3 added will inhibit the crystallization rates of cordierite and anorthite.

References

[1] S.H. Knickerbocker, A.H. Kumar, L.W. Herron, Am. Ceram. Soc. Bull. 72 (1993) 90.
[2] M. Sales, J. Alarcon, Journal of Mater. Sci. 30 (1995) 2341.
[3] J.J. Shyu, J.M. Wu, Journal of Mater. Sci. 29 (1994) 3167.
[4] W. Zdaniewski, Journal of Mater. Sci. 8 (1973) 192.
[5] M.G.M.U. Ismail, H. Tsunatori, Z. Nakai, Journal of Am. Ceram. Soc. 73 (1990) 537.
[6] R.W. Dupon, R.L. McConville, D.J. Musolf, A.C. Tanous, M.S. Thompson, Journal of Am. Ceram. Soc. 73 (1990) 335.
[7] C.F. Yang, Journal of Mater. Sci. Let. 15 (1996) 1618.
[8] M. Sales, J. Alarcon, Journal of Mater. Sci. 29 (1994) 5153.
[9] K. Kondo, M. Okuyama, Y. Shibata, in: J.B. Blum, R. Cannon (Eds.), Advances in Ceramics. vol. 19, American Ceramics Society, OH, USA, 1986, pp. 77–89.
[10] D.M. Miller, US Patent 3926648, 1975.
[11] W. Zdaniewski, Journal of Am. Ceram. Soc. 58 (1975) 163.
[12] A.H. Kumar, P.W. McMillan, R.R. Tummala, US Patent 4301324, 1981.
[13] W.D. Kingery, H.K. Bowen, D.R. Uhlmann, Introduction to Ceramics, Wiley & Sons, New York, 1976, p. 492.
[14] E.A. Giess, J.P. Flectcher, L.W. Herron, Journal of Am. Ceram. Soc. 69 (1984) 549.
[15] S.L. Fu, L.S. Chen, J.H. Chou, Ceram. Inter. 20 (1994) 67.
[16] E.A. Giess, S.H. Knickerbocker, Journal of Mater. Sci. Let. 4 (1985) 835.
[17] P.C. Panda, W.M. Mobley, R. Raj, Journal of Am. Ceram. Soc 72 (1989) 2361.
[18] R.C. Buchanan, in: R.C. Buchanan (Ed.), Ceramic Materials for Electronics, Marcel Dekker, New York, 1986, pp. 8–20.